The Astrophysical Journal, 663:677–685, 2007 July 1

MID-INFRARED SELECTION OF BROWN DWARFS AND HIGH-REDSHIFT QUASARS

Daniel Stern,[1] J. Davy Kirkpatrick,[2] Lori E. Allen,[3] Chao Bian,[4] Andrew Blain,[4] Kate Brand,[5] Mark Brodwin,[1] Michael J. I. Brown,[6] Richard Cool,[7] Vandana Desai,[4] Arjun Dey,[8] Peter Eisenhardt,[1] Anthony Gonzalez,[9] Buell T. Jannuzi,[8] Karin Menendez-Delmestre,[4] Howard A. Smith,[3] B. T. Soifer,[4,10] Glenn P. Tiede,[11] and E. Wright[12]

Received 2006 August 25; accepted 2006 November 15

ABSTRACT

We discuss color selection of rare objects in a wide-field multiband survey spanning from the optical to the mid-infrared. Simple color criteria simultaneously identify and distinguish two of the most sought after astrophysical sources: the coolest brown dwarfs and the most distant quasars. We present spectroscopically confirmed examples of each class identified in the IRAC Shallow Survey of the Boötes field of the NOAO Deep Wide-Field Survey. IRAC J142950.8+333011 is a T4.5 brown dwarf at a distance of approximately 30–40 pc, and IRAC J142738.5+331242 is a radio-loud quasar at redshift $z = 6.12$. Our selection criteria identify a total of four candidates over 8 deg^2 of the Boötes field. The other two candidates are both confirmed $5.5 < z < 6$ quasars, previously reported by Cool et al. (2006). We discuss the implications of these discoveries and conclude that there are excellent prospects for extending such searches to cooler brown dwarfs and higher redshift quasars.

Subject headings: galaxies: high-redshift — quasars: individual (IRAC J142738.5+331242) — stars: individual (IRAC J142950.8+333011) — stars: low-mass, brown dwarfs — surveys

Online material: color figures

1. INTRODUCTION

Wide-area surveys are one of the most powerful tools for observational astronomy and have led to discoveries ranging from Earth-crossing asteroids to the most distant quasars. Historically, when technology allows a wavelength regime to be newly probed, either in terms of sensitivity or area, one of the first tasks is a large shallow survey to see what astrophysical phenomena lurk in the uncovered territory. In recent years, major advances from this line of research include the discovery of the coolest Galactic stars by the Two Micron All Sky Survey (2MASS), ultraluminous infrared galaxies by the *Infrared Astronomical Satellite*, the most distant quasars by the Sloan Digital Sky Survey (SDSS), and the power spectrum of the cosmic microwave background, first by the *Cosmic Background Explorer* and later refined by the *Wilkinson Microwave Anisotropy Probe*. Such fundamental scientific discoveries have been a major incentive and reward for NASA's Explorer program and other large projects. The pace of scientific discovery relies on such programs continuing.

The mid-infrared regime has been made newly accessible by the launch of the *Spitzer Space Telescope* (Werner et al. 2004). At its least competitive, shortest wave band, 3.6 μm, *Spitzer* is still more than 5 orders of magnitude more efficient than the largest ground-based observatories for areal surveys. For the longest wave bands, ground-based observations are simply not possible. Even compared to previous space-based missions, *Spitzer* offers several orders of magnitude increase in mapping efficiency.

Thus inspired, we have undertaken a shallow, wide-area 3.6–8.0 μm survey with *Spitzer*, summarized in § 2. We discuss two of the rare, interesting astronomical sources which are ideally suited to selection by combining deep optical data with shallow mid-infrared data: the coolest Galactic brown dwarfs and the most distant quasars. The former, of course, are not actually rare in the cosmos; their faint optical magnitudes merely delayed their discovery until recent years and continue to make them "rare" in terms of known, spectroscopically confirmed examples. Section 3 discusses the selection criteria used to identify such sources and § 4 describes our spectroscopic observations, which confirmed both a cool brown dwarf (spectral class T4.5) and a high-redshift ($z = 6.12$) quasar. The implications for these discoveries are described in § 4, and § 5 summarizes the results and discusses future prospects. Throughout we adopt a $(\Omega_m, \Omega_\Lambda) = (0.3, 0.7)$ flat cosmology and $H_0 = 70$ km s^{-1} Mpc^{-1}. Unless otherwise stated, all magnitudes are quoted in the Vega system.

2. MULTIWAVELENGTH SURVEYS OF BOÖTES

The Boötes field is a 9 deg^2 field, which has been the target of deep observations across the electromagnetic spectrum. Boötes was initially selected as the north Galactic field of the NOAO Deep Wide-Field Survey (NDWFS; Jannuzi & Dey 1999), which obtained deep optical ($B_W RI$) and moderately deep near-infrared (K_s) images across the entire field.[13] These images reach

[1] Jet Propulsion Laboratory, California Institute of Technology, Pasadena, CA 91109; stern@zwolfkinder.jpl.nasa.gov.
[2] Infrared Processing and Analysis Center, California Institute of Technology, Pasadena, CA 91125.
[3] Harvard-Smithsonian Center for Astrophysics, Cambridge, MA 02138.
[4] Division of Physics, Math, and Astronomy, California Institute of Technology, Pasadena, CA 91125.
[5] Space Telescope Science Institute, Baltimore, MD 21218.
[6] Princeton University Observatory, Peyton Hall, Princeton University, Princeton, NJ 08544.
[7] Steward Observatory, University of Arizona, Tucson, AZ 85721.
[8] National Optical Astronomy Observatory, Tucson, AZ 85719.
[9] Department of Astronomy, University of Florida, Gainesville, FL 32611.
[10] *Spitzer* Science Center, California Institute of Technology, Pasadena, CA 91125.
[11] Department of Physics and Astronomy, Bowling Green State University, Bowling Green, OH 43403.
[12] Department of Physics and Astronomy, University of California at Los Angeles, Los Angeles, CA 90095.

[13] The third data release is publicly available at http://www.archive.noao.edu/ndwfs . The optical filter specifications are B_W ($\lambda_c = 4111$ Å, FWHM = 1275 Å), R ($\lambda_c = 6514$ Å, FWHM = 1511 Å), and I ($\lambda_c = 8205$ Å, FWHM = 1915 Å). The R and I filters are part of the Harris filter set, and the photometry was calibrated to match the Cousins system. The FLAMEX near-infrared filter specifications are J ($\lambda_c = 1.25$ μm, FWHM = 0.16 μm; similar to the Mauna Kea Observatory J-band filter) and K_s ($\lambda_c = 2.15$ μm, FWHM = 0.30 μm; similar to the 2MASS K_s-band filter).

approximate 5 σ point-source depths of $B_W = 27.1$, $R = 26.1$, $I = 25.4$ (B. T. Jannuzi et al. 2007, in preparation) and $K_s = 19.0$ (A. Dey et al. 2007, in preparation). Subsequently, the field has been observed at X-ray energies with the *Chandra X-Ray Observatory* (Murray et al. 2005), with a z' filter using the Bok 2.3 m telescope at Kitt Peak (Cool 2007), more deeply in the near-infrared (JK_s) as part of the FLAMINGOS Extragalactic Survey (FLAMEX; Elston et al. 2006), in the infrared with the *Spitzer Space Telescope* (Eisenhardt et al. 2004; Papovich et al. 2004), and at radio frequencies using the Westerbork Synthesis Radio Telescope (1.4 GHz; de Vries et al. 2002) and the Very Large Array (325 MHz; S. Croft et al. 2007, in preparation). Approximately 20,000 spectroscopic redshifts in the Boötes field have been obtained by the AGN and Galaxy Evolution Survey (AGES; C. Kochanek et al. 2007, in preparation), and Brodwin et al. (2006) reports on nearly 200,000 photometric redshifts in this field.

The mid-infrared imaging of Boötes is central to this paper. As part of a guaranteed-time observation program, 8 deg^2 of the field was imaged with the Infrared Array Camera (IRAC; Fazio et al. 2004) at 3.6–8 μm. Eisenhardt et al. (2004) presents the survey design, reduction, calibration, and initial results. The survey, called the IRAC Shallow Survey, identifies ≈270,000, 200,000, 27,000, and 26,000 sources brighter than 5 σ Vega magnitude limits of 18.4, 17.7, 15.5, and 14.8 at 3.6, 4.5, 5.8, and 8.0 μm, respectively, where IRAC magnitudes are measured in 6″ diameter apertures and corrected to total magnitudes assuming sources are unresolved at the 1.66″–1.98″ resolution of IRAC.

3. MID-INFRARED SELECTION OF RARE SOURCES

Two core science goals of the IRAC Shallow Survey are the identification of the coolest brown dwarfs and the identification of the most distant quasars. Both are optically faint sources that are difficult to find, but are highly sought after for their astrophysical significance. Brown dwarfs probe the stellar-to-planetary link (e.g., Kirkpatrick 2005), while the highest redshift quasars probe the conditions of the early universe and the onset of cosmic reionization (e.g., Fan et al. 2006). Currently, there are less than 100 T-type brown dwarfs known and only 10 quasars at $z > 6$. Both brown dwarfs and the most distant quasars are substantially brighter at mid-infrared wavelengths than at optical wavelengths. Therefore, wide-area, shallow infrared surveys are ideally suited to identifying samples of both types of sources.

Brown dwarfs have red optical colors due to their cool temperatures. At mid-infrared wavelengths the spectra of *most* stars generally follow a Rayleigh-Jeans tail, giving them mid-infrared Vega colors near zero. For cooler stars and brown dwarfs, however, the presence of deep molecular absorptions results in very different emergent spectra (Kirkpatrick 2005). Specifically, the fundamental bands of CH_4 and CO between 3 and 5 μm (Oppenheimer et al. 1998; Cushing et al. 2005) and additional bands of H_2O, CH_4, and NH_3 between 5 and 12 μm (Roellig et al. 2004) dramatically recarve the spectral energy distributions (SEDs) of these objects and give them unique IRAC colors (Patten et al. 2006). Shortward of 3 μm, H_2O bands in L and T dwarfs (and CH_4 bands in T dwarfs only) cause deep depressions in the near-infrared spectra (e.g., Geballe et al. 2002; McLean et al. 2003), and pressure-broadened Na I and K I resonance doublets suppress much of the flux below 1 μm (Kirkpatrick et al. 1999; Burgasser et al. 2003a), making brown dwarfs extremely faint in the optical. Specifically, the colors of known brown dwarfs later than type mid-T are $R - I > 3.5$ (Kirkpatrick et al. 1999; Dahn et al. 2002), $0.7 < [3.6] - [4.5] < 2$, and $0 < [5.8] - [8.0] < 0.8$ (Patten et al. 2006).

High-redshift quasars have red colors primarily due to absorption by foreground neutral hydrogen in the intergalactic medium, which strongly suppresses the intrinsic UV emission of these AGNs. At the highest redshifts, $z \gtrsim 6$, very little flux is detectable below Lyα, providing the highest redshift quasars with similar optical colors to cool stars. Longward of Lyα, luminous quasars are well approximated by a power law and are easily identified in mid-infrared color-color diagrams (e.g., Stern et al. 2005).

Therefore, both the coolest brown dwarfs and the highest redshift quasars should easily be identifiable by selecting unresolved sources with very red optical colors and relatively flat (in f_ν) mid-infrared SEDs. Figure 1 illustrates these selection criteria for the Boötes field. Note that at the highest redshifts, $z > 7$, quasars drop out of the optical completely. Typical colors of optical (I-band) point sources are presented. These color-color plots clearly separate stars and quasars, at least for typical hot stars and typical moderate-redshift quasars: most stars have mid-infrared colors near zero, while quasars are distinguished by their redder mid-infrared colors. Three confirmed quasars in this field at $5.39 \leq z \leq 5.85$, identified by Cool et al. (2006), are indicated, as are twelve $z \approx 6$ quasars from the SDSS (Jiang et al. 2006). The IRAC color criteria empirically determined by Stern et al. (2005) and Cool et al. (2006) to select luminous AGNs are indicated. In addition, the colors of M, L, and T dwarfs from Dahn et al. (2002) and Patten et al. (2006) are plotted. The thick solid line shows the expected colors of $3 \leq z \leq 7$ quasars, calculated using the Richards et al. (2006) SDSS quasar template subject to the Madau (1995) formulation for the opacity of the intergalactic medium as a function of redshift. As can be seen, the Lyα forest causes high-redshift quasars to become very red in $R - I$ at $z \gtrsim 5$, while the mid-infrared colors vary only slightly over this large redshift range. Cool stars and high-redshift quasars are identifiable from their red $R - I$ and [3.6]−[4.5] colors. Longer wavelength [5.8]−[8.0] colors can provide additional information, but require deeper data to obtain robust detections in these less sensitive passbands.

As seen in Figure 1, both brown dwarfs and high-redshift quasars should be easily identified using the simple (Vega-system) selection criteria of (1) $R - I \geq 2.5$, (2) $[3.6] - [4.5] \geq 0.4$, and (3) unresolved at I band. To restrict the number of spurious sources identified in the catalogs, we also require (4) $B_W - I \geq 2.5$. These constraints implicitly require robust detections (≥ 5 σ) or robust nondetections in the various bands; e.g., we require that candidates all reside in areas of the survey with good optical, 3.6 and 4.5 μm coverage. In particular, the I-band morphology criterion requires $I \lesssim 23$ for the NDWFS survey, which has typical I-band seeing of 1.05″.

We estimate that our selection criteria restrict our sensitivity to brown dwarfs of spectral type T3 to T6 and to quasars at $5.5 \lesssim z \lesssim 6.5$. The high-temperature brown dwarf limit comes from the IRAC color criterion (Patten et al. 2006), and the cool temperature brown dwarf limit comes from available data suggesting that I-band flux drops dramatically for spectral types cooler than T6 (J. D. Kirkpatrick et al. 2007, in preparation). For quasars, the lower redshift limit comes from the $R - I$ color requirement, determined from the Richards et al. (2006) model discussed above; indeed, the $z = 5.39$ quasar identified by Cool et al. (2006) is too blue in $R - I$ to meet our selection criteria (Fig. 1). The upper redshift limit corresponds to Lyα shifting out of the I-band filter.

The Boötes 4.5 μm catalog (ver. 1.3) identifies 22 candidates matching these selection criteria, which are trimmed to four robust candidates after visual inspection. The most common cause of a false positive is source blending. One source, IRAC J142918.1+343731, appeared modestly robust after visually inspecting the ground-based imaging. However, the source resides near a $z > 1$

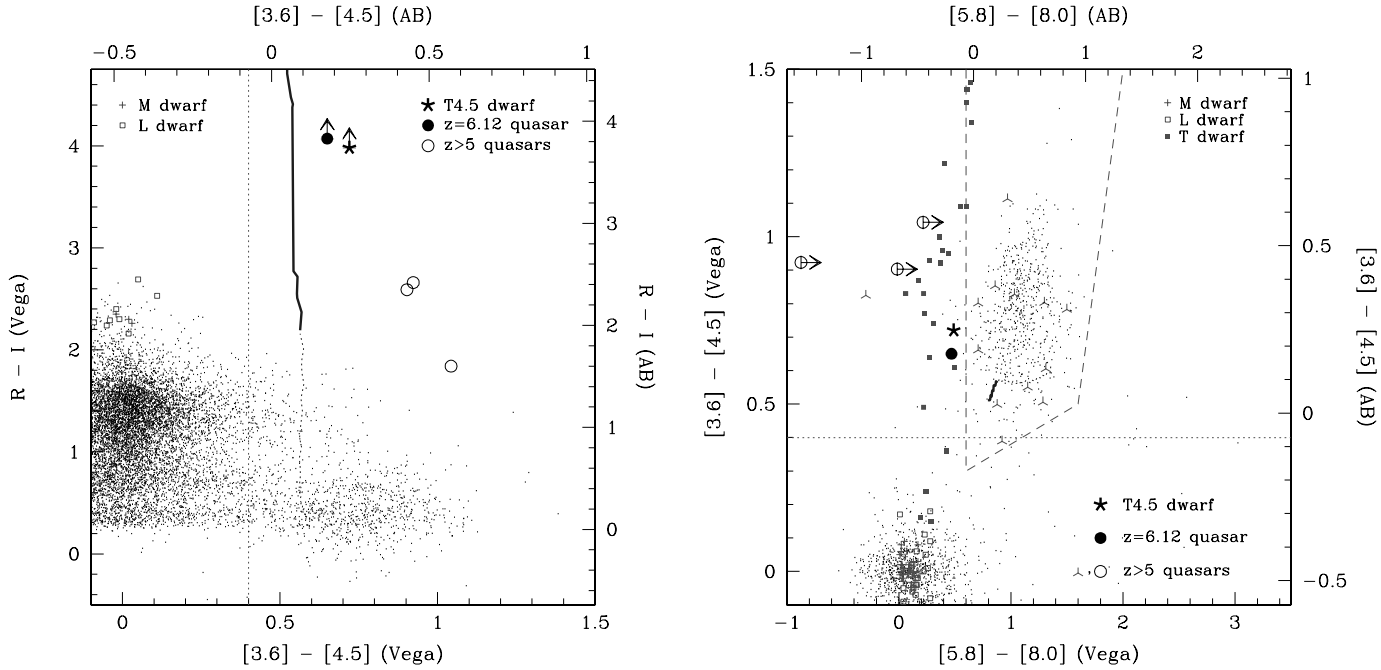

FIG. 1.—Color-color diagrams for unresolved sources in the Boötes field. As indicated, the asterisk refers to IRAC J142950.8+333011 (T4.5 brown dwarf), the filled circle refers to IRAC J142738.5+331242 ($z = 6.12$ quasar), and the open circles refer to Boötes field $5 < z < 6$ quasars from Cool et al. (2006). The dashed line in the right panel illustrates the empirically determined wedge largely populated by luminous, unobscured AGNs (Stern et al. 2005b). The dotted line illustrates the selection criteria employed in Cool et al. (2006) to identify luminous AGNs, which are too faint to be detected in all IRAC channels, $[3.6] - [4.5] > 0.4$. Dots illustrate typical colors of sources that are unresolved in the *I* band (stellarity index ≥ 0.8). In the left panel, sources with $18 \leq I \leq 21$ and $\geq 5\,\sigma$ detections in [3.6] and [4.5] are plotted. In the right panel, sources with $10 \leq I \leq 20$ and $\geq 5\,\sigma$ detections in all four IRAC passbands are plotted. Photometry of M, L, and T dwarfs from Dahn et al. (2002; optical) and Patten et al. (2006; IRAC) are the open squares, filled squares, and plus signs, as indicated. SDSS quasars at $z \approx 6$ are plotted as inverted Y's (Jiang et al. 2006). Quasars and typical stars are clearly separated on the basis of their mid-infrared colors. The black line illustrates the colors of the SDSS quasar template from Richards et al. (2006) for $3 \leq z \leq 7$, subject to the Madau (1995) formulation for the opacity of the intergalactic medium as a function of redshift. The line becomes thicker for $z \geq 5.5$. [*See the electronic edition of the Journal for a color version of this figure.*]

galaxy cluster identified by P. Eisenhardt et al. (2007, in preparation). *Hubble Space Telescope* imaging of the cluster (GO 10836; PI S. Perlmutter) shows that the potential candidate is compact, but clearly resolved, and thus unlikely to be either a brown dwarf or a high-redshift quasar. Two of the final four candidates have already been spectroscopically confirmed as $5.5 < z < 6$ quasars by Cool et al. (2006). The remaining two were targeted spectroscopically during Spring 2006, as discussed next. Table 1 presents all four Boötes field candidates in order of decreasing 3.6 μm flux, and Figure 2 presents finding charts for the two new sources described in § 4. We note that the $I < 23$ requirement imposed to provide robust morphological selection of unresolved sources is a very significant limiting factor for this survey. For example, for the first candidate, IRAC J142950.8+333011, the 4.5 μm flux is 2.7 mag brighter than the survey limit (i.e., $V/V_{\max} = 0.024$), whereas the *I* magnitude is only 0.9 mag above the limit ($V/V_{\max} = 0.3$). In § 5 we discuss the results of relaxing some of the selection criteria.

4. SPECTROSCOPIC OBSERVATIONS AND DISCUSSION

Initial spectroscopic follow-up of candidates was obtained with the Multi-Aperture Red Spectrometer (MARS; Barden et al. 2001) on the Mayall 4 m telescope at Kitt Peak. MARS is an optical spectrograph that uses a high resistivity, p-channel Lawrence Berkeley National Laboratory CCD with little fringing and very high throughput at long wavelengths ($8500 \lesssim \lambda \lesssim 10500$ Å). On the nights of UT 2006 March 24–26, we obtained spectra of red sources in the Boötes field using the 1.7″ wide long slit, OG550 order-sorting filter, and the VG8050 grism. Across much of the optical window the instrument configuration provides resolution $R \approx 1100$ spectra, as measured from sky lines filling the slit. IRAC J142950.8+333011 was observed for 1.5 hr on UT 2006 March 24, split into three dithered 1800 s exposures. IRAC J142738.5+331242 was observed for 1 hr on UT 2006 March 25, split into three 1200 s exposures. The data were processed following standard optical slit spectroscopy procedures. The nights were not photometric, but relative flux calibration of the spectra was achieved with observations of the spectrophotometric standards Feige 34 and PG 0823+546 (Massey & Gronwall 1990) obtained during the same observing run. The extracted, calibrated MARS spectra are presented in Figures 3 and 4. The bright star 3.3″ east of IRAC J142738.5+331242 made extraction of the fainter target challenging, resulting in systematic fluctuations of the background at the 10 μJy level.

Near-infrared spectroscopy of IRAC J142950.8+333011 was obtained with the cryogenic cross-dispersed Near-Infrared Echelle Spectrograph (NIRSPEC; McLean et al. 1998) on the Keck II 10 m telescope atop Mauna Kea. We first obtained *J*- and *H*-band spectroscopy on UT 2006 April 5. An AB nod sequence with a total on-source integration time of 200 s per grating setting was used. For both grating settings, the G2 V star GSPC P300-E from Colina & Bohlin (1997) was used for both telluric correction and flux calibration. An additional *J*-band spectrum was acquired on UT 2006 May 11. On this night 300 s integrations were taken both on-source and off-source, and the F0 star BD +66 1089 was acquired for telluric correction and flux calibration. All NIRSPEC observations used the 0.76″ wide slit, which provides resolution $R \approx 1400$ spectra. Figure 5 presents the combined near-infrared spectrum.

4.1. *IRAC J142950.8+333011: Mid-T Brown Dwarf*

The spectrum of IRAC J142950.8+333011 shows the classic signatures of a T dwarf. The optical spectrum in Figure 3 shows

TABLE 1

PHOTOMETRY OF BOÖTES FIELD CANDIDATES

Target	B_W	R	I	z'	J	K_s	[3.6]	[4.5]	[5.8]	[8.0]	Notes
IRAC J142950.8+333011.....	>27.1	>26.1	22.12 ± 0.09	21.22 ± 0.07	16.88 ± 0.03	16.99 ± 0.04	15.76 ± 0.03	15.04 ± 0.03	15.05 ± 0.16	14.56 ± 0.16	T4.5 dwarf
IRAC J142738.5+331242.....	>27.1	>26.1	22.03 ± 0.09	...	19.83 ± 0.05	18.17 ± 0.05	16.57 ± 0.04	15.92 ± 0.05	15.28 ± 0.19	14.81 ± 0.20	$z = 6.12$
IRAC J142729.6+352209.....	>27.1	23.99 ± 0.39	21.38 ± 0.05	22.47 ± 0.13	...	18.44 ± 0.19	17.33 ± 0.08	16.70 ± 0.09	>15.5	>14.8	$z = 5.53$
IRAC J142516.3+325409.....	>27.1	23.76 ± 0.21	21.15 ± 0.04	21.22 ± 0.06	...	...	17.41 ± 0.08	16.77 ± 0.09	>15.5	>14.8	$z = 5.85$

NOTES.—Brown dwarf and high-redshift quasar candidates in the Boötes field, listed in order of 3.6 μm brightness. Astrometry, used for the nomenclature, is derived from the 4.5 μm images (obtained during UT 2004 January 10–14). The first two sources are discussed in detail here; the latter two are discussed in Cool et al. (2006). Photometry is all Vega-based, total magnitudes (filter specifications are provided in footnote 13 of § 2). Optical photometry is from the NDWFS ($B_W RI$; B. T. Jannuzi, et al. 2007, in preparation) and zBoötes (z'; Cool 2007). Near-infrared photometry is from FLAMEX (JK_s; Elston et al. 2006). Mid-infrared photometry is from the IRAC Shallow Survey (Eisenhardt et al. 2004). Nondetection limits are the average 5 σ limits for the relevant bands across the entire field. Ellipses indicate sources that were either not observed at a wave band or had bad coverage in that wave band. Catalogued FLAMEX near-infrared photometry for the $z = 6.12$ quasar was corrupted by the bright, neighboring star. Photometry above comes instead from DAOPHOT analysis of the images, using stars in the field to model the PSF.

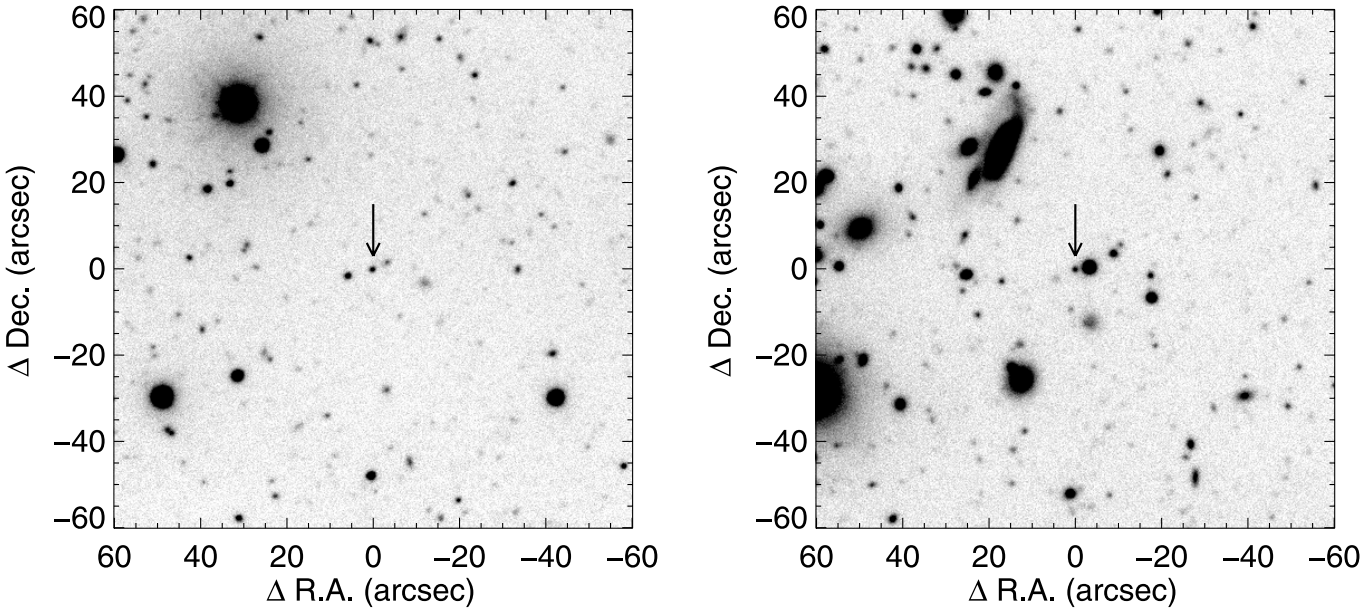

FIG. 2.—Finding charts for IRAC J142950.8+333011 (T4.5 brown dwarf) and IRAC J142738.5+331242 ($z = 6.12$ quasar) from the NDWFS *I*-band imaging. The fields are $2' \times 2'$ centered on the targets. North is at the top, and east is to the left.

a sharp rise to the longest wavelengths, indicative of a cool temperature and strong absorption by the pressure-broadened wings of K I (and to some extent Na I). Even more telling are the *J*- and *H*-band spectra in Figure 5 that show strong CH_4 and H_2O absorption, the former of which is the hallmark of spectral class T.

As this object has both optical and near-infrared spectra, we can classify it with both the optical and near-infrared classification schemes. The optical typing of T dwarfs is somewhat crude because the ≤ 1 μm spectra show less variation than at longer wavelengths. Nonetheless, Burgasser et al. (2003a) have established standards for classes T2, T5, T6, and T8. In the 6000–10000 Å range the best diagnostic is the 9300 Å band of H_2O. Unfortunately, our MARS spectrum has not been telluric corrected, so the depth of this water feature will be influenced by both the earth's atmosphere as well as the atmosphere of the brown dwarf itself. This feature in IRAC J142950.8+333011 is not as deep as in the spectrum of a T8, so the true spectral type must be earlier than that. Comparisons with the T2, T5, and T6 standards obtained with Keck (Burgasser et al. 2003a) show that the overall slope most resembles that of the T5. Given the coarseness of classification in this wavelength regime, we can assign only a crude optical spectral type of T5 $\pm$ 2.

In the near-infrared, the situation is much improved. In this wavelength regime there is a full set of standards for each spectral subtype from T0 to T8 (Burgasser et al. 2006). Using Keck NIRSPEC spectra from McLean et al. (2003) of the Burgasser et al. (2006) standards, we find that the individual *J*-band spectra

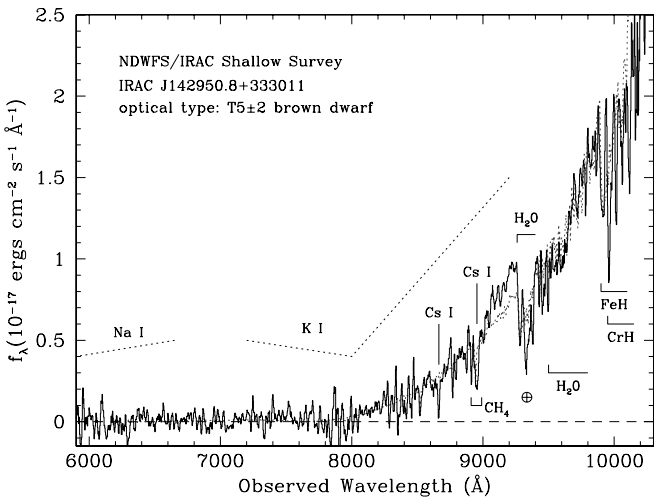

FIG. 3.—Optical spectrum of IRAC J142950.8+333011, optically classified as a T5 $\pm$ 2 brown dwarf, obtained with the MARS spectrograph on KPNO 4 m telescope. The relative flux calibration was determined from observations of standard stars from the same observing runs with the same instrumental configurations. The spectrophotometric scale was estimated from the imaging. The dotted spectrum shows 2MASS J0559−1404, classified as a T5 brown dwarf at optical wavelengths (Burgasser et al. 2003a). [*See the electronic edition of the Journal for a color version of this figure.*]

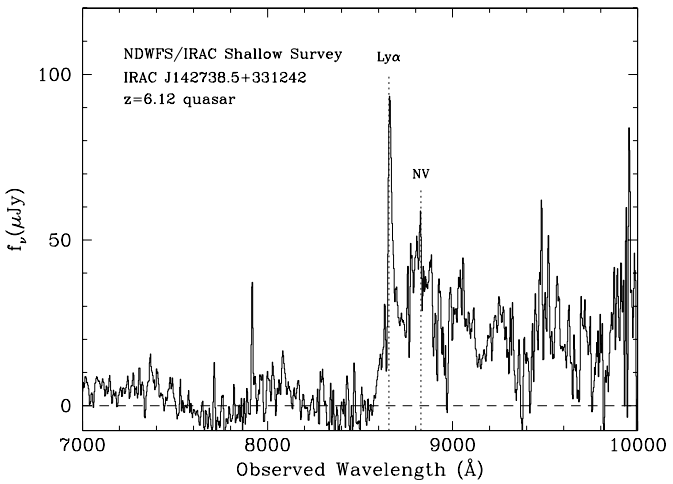

FIG. 4.—Spectrum of IRAC J142738.5+331242, a quasar at $z = 6.12$, obtained with the MARS spectrograph on the Kitt Peak 4 m Mayall telescope. The relative flux calibration was determined from observations of standard stars from the same observing run with the same instrumental configuration. As the nights were not photometric, the spectrophotometric scale has been estimated from the imaging. The bright star 3.3″ east of the quasar made extraction challenging, causing systematic fluctuations of the background at the 10 μJy level.